Trap-limited hole mobility in semiconducting poly(3-hexylthiophene)

Z. Chiguvare* and V. Dyakonov†
University of Oldenburg, Department of Energy and Semiconductor Research, Institute of Physics, D-26111 Oldenburg, Germany
(Received 26 February 2004; revised manuscript received 23 August 2004; published 15 December 2004)

Bulk transport properties of poly(3-hexylthiophene) (P3HT) were studied by analyzing temperature dependent current-voltage characteristics of the polymer thin films sandwiched between indium tin oxide/polystyrene sulfonate doped polyethylene dioxy-thiophene (ITO/PEDOT) and aluminium electrodes. It was found that the contacts limit charge injection under reverse bias, but under forward bias the current is limited by space charge that accumulates near the hole injecting electrode (ITO/PEDOT) resulting in a rectification of 10^5. The forward current density obeys a power law of the form $J \sim V^m$, with $m > 2$, described by space charge limited current in the presence of exponentially distributed traps within the band gap. In this paper we describe the deduction, and discuss the limits, of an expression for the calculation of the total trap density, based on the exponential trap distribution model, which yielded reasonable agreement with our experimental $J(V)$ data. The total deep hole trap density was estimated to be 3.5×10^{16} cm^{-3}, and the activation energy extrapolated to zero Kelvin was obtained to be 0.054 eV. Temperature dependent hole mobility in P3HT was also estimated under trap-free space charge conditions, yielding a value of 3×10^{-5} cm^2/V s, at 304 K.

DOI: 10.1103/PhysRevB.70.235207 PACS number(s): 72.80.Le, 73.50.Gr, 73.61.Ph

I. INTRODUCTION

A. Motivation

Conjugated polymers are interesting materials for the fabrication of electronic devices such as light emitting diodes[1] solar cells,[2,3] and thin film field effect transistors[4] on flexible substrates. Poly(3-hexylthiophene) (P3HT) has emerged as one of the very promising materials and is currently a subject of intense research. It has demonstrated promising physical properties, for example, a good stability, reasonably high hole mobility in the range of 10^{-3} cm^2 V^{-1} s^{-1} (Ref. 5) and a field effect mobility, which can be as high as 0.1–0.2 cm^2 V^{-1} s^{-1} in high quality self-organized samples.[6–8] For instance, power conversion efficiencies of solar cells based on P3HT-fullerene blends of up to 3.5% have been reported,[9,10] while P3HT field effect transistors reaching on-off current ratios of $>10^6$ have been achieved.[11] However the physics of devices based on P3HT is not yet fully understood.

The understanding of the basic physics underlying the electrical, thermal, and optical behavior of organic polymeric materials is essential for the optimization of devices fabricated using these materials. We report a study of the electrical properties of spin-cast P3HT films sandwiched between ITO/PEDOT and Al electrodes by analyzing their $J(V)$ characteristics. The nonlinear $J(V)$ curves are described using the space charge limited current (SCLC) model in the presence of exponentially distributed hole traps within the band gap of P3HT. The characteristic hole trap depths were quantified for each temperature, then used to obtain the activation energy, the total trap density, and the quasi-Fermi levels in the P3HT films.

B. Theory

The classical mechanism of the dark charge carrier injection depends on the potential barrier at the interface and on the temperature dependent energy of electrons incident on that barrier. Alternatively,[12] the injection by means of the thermally assisted hopping of charge carriers from the metal electrode into localized electronic states of the polymer may occur. Once charge carriers are injected, their transport through the polymer layer towards the adjacent electrode under the influence of the external electric field is determined by the conduction properties of the material itself. For low bias the number of injected carriers is smaller or comparable to the thermally generated intrinsic charge carriers, and the current-voltage characteristics can be described by Ohm's law. The space charge limited current (SCLC) model[13,14] describes charge transport in a low conductivity material, where the concentration of injected charge may exceed the intrinsic charge concentration, and space charge builds up in the sample. The application of this model provides useful material characteristics such as the trap distribution in the energy band gap, the position of the Fermi energy, and charge carrier mobility.

Investigations have shown that bulk conduction in disordered, and that in undoped, conjugated polymers is also described well by the hopping transport of electrons and holes, taking into account space charge effects and traps of different depths.[15] The conformational disorder in conjugated polymers is well approximated by the Gaussian function. Whereas the pure exponential shape of the distribution of states (DOS) is widely assumed for amorphous materials, the Gaussian DOS is usually assumed for random organic solids such as polymers.[16]

The concept of transport level (or energy) remains, however, valid for Gaussian and Gaussian-type DOS, as it does in pure exponential case. As discussed by Campbell *et al.*,[17] the Gaussian and exponential distributions are almost indistinguishable in SCLC conduction regime. They showed that the SCLC model with field independent mobility, in presence of exponentially distributed traps gives qualitatively the same results as trap free SCLC with a field dependent mobility of the Poole-Frenkel type.[18–20]

 ©2004 The American Physical Society

Current density-voltage $[J(V)]$ characteristics of electrode/polymer/electrode devices can often be fitted excellently by the power law $J\sim V^m$ with $m>2$, characteristic of the filling of exponentially distributed traps.[21] Traps may originate from structural defects or due to perturbed molecules in the lattice causing charge of polarization energy in the perturbed regions, which may also tend to lower the bottom edge of the conduction band, or to raise the bottom edge of the valence band. We used the exponential DOS due to the simplicity of the solution. In the following section we briefly describe the exponential trap distribution model, and deduce an expression for the calculation of the total trap density, which yielded reasonable agreement with our experimental $J(V)$ data.

C. Exponential distribution of traps

We consider a hole-only device for the following description, and note that the reverse will be equally true for electron only devices. The distribution function for the hole trap density as a function of energy level E above the valence band, and a distance x from the injecting contact for holes can be written as[13]

$$h(E,x)=n(E)s(x), \tag{1}$$

where $n(E)$ and $s(x)$ represent the energy, and spatial, distribution functions of traps, respectively. An assumption of uniform spatial trap distribution within the specimen from injecting electrode to collecting electrode implies that the effective thickness of the device, under space charge conditions, remains the thickness itself, and $s(x)=1$. The specific functional form of the SCLC current density versus voltage, $J(V)$ curve depends on the distribution of charge traps in the band gap.

For traps that are exponentially distributed within the energy band gap, Eq. (1) becomes

$$h(E)=n(E)=\frac{N_{vb}}{E_t}\exp\left(-\frac{E}{E_t}\right), \tag{2}$$

which can be written as

$$N(E)=N_{vb}\exp\left(-\frac{E}{E_t}\right), \tag{3}$$

where $N(E)=n(E)E_t$ is the trap density at an energy level E above the valence band edge, and N_{vb} is the trap density at the valence band edge; E_t is the characteristic constant of the distribution, also often expressed as a characteristic temperature T_t ($E_t=k_BT_t$), where k_B is Boltzmann's constant. Equation (2) assumes that the maximum number of traps is located at the valence band edge, and decreases exponentially as we go deep into the energy band gap. To extract the physical significance of E_t, we consider the case when the trap energy $E=E_t$, therefore Eq. (2) can be simplified as

$$\frac{N(E_t)}{N_{vb}}=\frac{1}{e}=\text{constant}. \tag{4}$$

Equation (4) states that the trap energy level that characterizes the exponential distribution is defined as the energy at which the density of traps has been reduced by $1/e$, as compared to the trap density at the valence band edge. The characteristic width of the exponential distribution is therefore set by the energy E_t. At the conduction band edge we expect the density of hole traps to vanish. In Eq. (2), $E=E_{cb}\gg E_t$, therefore, $N(E_{cb})\sim 0$, where E_{cb} is the energy level of the conduction band edge. The total density of traps in the distribution is given by $N_{\text{total}}=N_{vb}k_BT_t$.[22]

The exponential trap distribution [Eq. (3)] implies a power law dependence of current density on the bias voltage given by[13,14]

$$J=q^{1-l}\mu_pN_v\left(\frac{2l+1}{l+1}\right)^{1/l}\left(\frac{l}{l+1}\frac{\epsilon\epsilon_0}{N_{\text{total}}}\right)^l\frac{V^{l+1}}{d^{2l+1}}, \tag{5}$$

where q is the electronic charge, ϵ_0 is the permittivity of free space, ϵ is the dielectric constant of material, μ_p is charge carrier mobility of holes, N_v is the density of states in the valence band, N_{total} is the total density of traps; $l=T_t/T$, T is the measurement temperature in K, d is the sample thickness, $m=l+1$, and $J\sim V^m$ is the power law obtained. After performing some simple algebraic manipulations we rewrite Eq. (5) in its Arrhenius form to bring out the dependence of current density on temperature. Grouping together all the terms with l from Eq. (5), we obtain

$$J=\frac{q\mu_pN_vV}{d}\left[\left(\frac{2l+1}{l+1}\right)^{1/l}\frac{l(2l+1)}{(l+1)^2}\frac{\epsilon\epsilon_0V}{qd^2N_{\text{total}}}\right]^l. \tag{6}$$

We can apply the exponential function to a natural logarithm without altering the result, and when we consider that $l=T_t/T$ we obtain that Eq. (5) can be written as

$$J=\frac{q\mu_pN_vV}{d}\exp\left\{-\frac{E_t}{k_BT}\ln\left[\left(\frac{2l+1}{l+1}\right)^{-1/l}\frac{(l+1)^2}{l(2l+1)}\frac{qd^2N_{\text{total}}}{\epsilon\epsilon_0V}\right]\right\}. \tag{7}$$

Therefore, for an exponential distribution of traps, the quasi-Fermi level, which depends on the magnitude of stored charge and hence on the applied voltage is given by

$$E_F(V)=k_BT_t\ln\left[f(l)\frac{qd^2N_{\text{total}}}{\epsilon\epsilon_0V}\right], \tag{8}$$

with

$$f(l)=\left(\frac{2l+1}{l+1}\right)^{-1/l}\frac{(l+1)^2}{l(2l+1)}. \tag{9}$$

E_F is measured from the edge of the valence band for the hole injection, or from the conduction band edge for electron injection.

Kumar *et al.*[23] obtained a similar expression for E_F, which they called activation energy, by rewriting Eq. (5) to bring out the Arrhenius dependence of current density on temperature, resulting in that the prefactor with l is equal to 0.5, through some approximation within 4%. Kao and Huang[13] gave an expression for E_F similar to the one in Eq. (8), but without the factor raised to the power $(-1/l)$, possibly because they approximated that term to 1. In the analysis, by Tans *et al.*,[24] of the power law asymptotes of the $J(V)$ characteristics in presence of exponentially distributed traps one

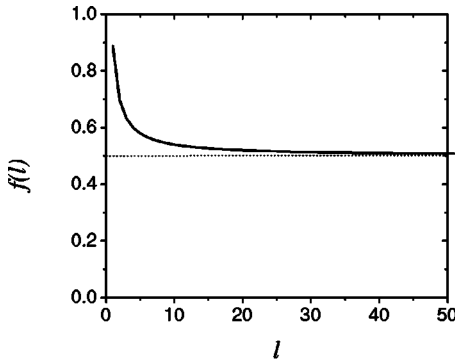

FIG. 1. Graph of $f(l)$ vs l, Eq. (9) for values of l from the minimum allowed $l=1$ to an arbitrary $l=50$. When l tends to infinity $f(l)$ tends to 0.5. $f(l)$ describes the limits of validity of the exponential trap distribution model.

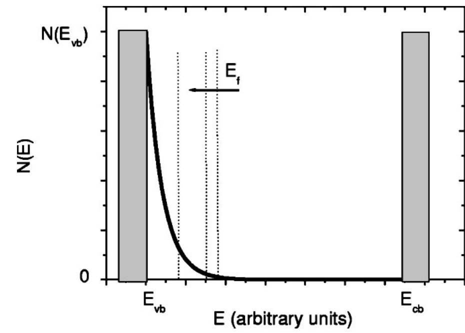

FIG. 2. Schematic diagram of the proposed exponentially distributed density of states as a function of energy, $N(E)$, at constant temperature. E_{vb} and E_{cb} mark the edges of the valence and conduction bands, respectively. In the band gap, the area under the bold exponential distribution curve indicates the total trap density. Upon application of a high electric field, space charge builds up in the sample, resulting in a shift of the Fermi energy E_F towards the valence band, and a corresponding increase in current.

can infer that they considered $f(l)$ to be equal to 1. To clarify the apparent lack of consistency, we discuss the permitted limits of the prefactor $f(l)$ in Eq. (9).

In Fig. 1 we show a graph of $f(l)$ vs l [Eq. (9)] for values of l from the minimum allowed $l=1$ (corresponding to $m=2$) to an arbitrary $l=50$.

Calculation shows that $f(l)$ decreases monotonously, e.g., from (8/9) to 0.51 for values of l between 1 and 30. In the limit when l tends to infinity, $f(l)$ tends to 0.5. We suggest that 0.5 is the value of $f(l)$ when the $J(V)$ curve in double logarithmic scale becomes vertical. In that case, the description of traps by a continuous exponential distribution ceases to be valid. The traps being filled are then described as being situated on some discrete energy level within the band gap.[13,14] When $f(l)$ is the maximum allowed value of (8/9), all traps are filled, and there is no trap filling taking place. This happens when $m=2$. We define therefore that the exponential description is valid if $0.5<f(l)<(8/9)$. Therefore using any of the two extremes in the calculation of E_F or N_{total} cannot be justified, worse approximating to a prohibited value 1, even if this will not alter the numerical result significantly. For values of $l<10$, which are usually obtained practically, one expects shallow traps close to the valence band edge, some of which in fact can be filled by thermal energy.

Figure 2 illustrates the effect of space charge on the Fermi level in the SCLC regime, at constant temperature.

Upon an increase of the bias voltage, the increased positive space charge will occupy the first available trap states for holes in the band gap, which corresponds to a shift of E_F towards the valence band edge.[24]

Further, we may rewrite Eq. (8) as

$$E_F(V) = k_B T_t \ln\left[f(l)\frac{qd^2 N_{\text{total}}}{\epsilon\epsilon_0} - \ln V \right], \tag{10}$$

where $f(l)$ is the prefactor with l in Eq. (9), and is constant for any given temperature, where the power law $J\sim V^m$, $m>2$ is satisfied. In the SCLC regime E_F is thus linearly dependent on $\ln V$. The Fermi level $E_F(V)$ will coincide with the valence band edge ($E_F=0$), only if the right-hand-side of Eq. (10) is zero. This takes place when the applied voltage, V, reaches a critical voltage given by

$$V = V_c = f(l)\frac{qd^2 N_{\text{total}}}{\epsilon\epsilon_0}. \tag{11}$$

At the bias voltage V_c all the traps are filled and E_F coincides with the valence band edge energy E_{vb}. V_c obtained for the temperature in question [implicitly expressed in the function $f(l)$] indicates the minimum voltage which is necessary to apply in order to fill up all existing traps at that temperature. Practically, we expect the slope of the $J(V)$ curve to transform itself to 2 as V_c is approached, in conformity with trap free SCLC. If V_c is the same for all temperatures, this indicates that the traps are so deep that at temperatures considered, the energies k_BT are smaller than those required to fill up any significant number of the traps. The variation of V_c, which is directly proportional to the total number of traps in the bulk, with temperature indicates the measure by which thermal energy fills up traps. At high temperatures we would expect more traps to be filled thermally than at low temperatures, and the fraction to be filled by voltage should be reduced. The slope of the $J(V)$ curves determined by Eq. (5) increases rapidly with decreasing temperature, making $f(l)$ smaller, thus increasing the fraction of the total number of traps that must be filled by injected charges due to applied voltage.

If the obtained trap distribution parameter $E_t=k_BT_t \gg k_BT$, then a crossover point is observed in the $\log J$-$\log V$ plot, where V_c and the corresponding current density, J_c, are independent of temperature. A plot of E_F vs $\ln V$ for different temperatures should yield straight lines that converge at $\ln V_c$. If such a crossover point is observed in measured $J(V)$ characteristics, one may then estimate the total deep trap density from Eq. (11), as

$$N_{\text{total}} = \frac{1}{f(l)}\frac{\epsilon\epsilon_0 V_c}{qd^2}, \tag{12}$$

with $0.5<f(l)<(8/9)$. The total trap density in the exponential distribution is therefore greatest for large l, (low T),

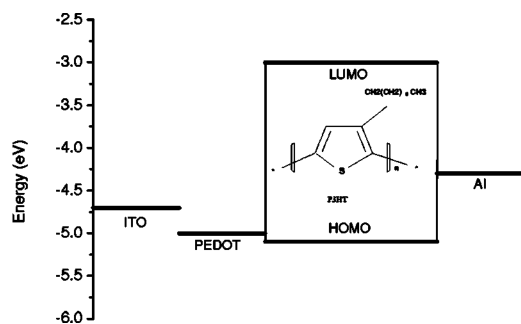

FIG. 3. Formula of poly(3-hexylthiophene), and important energy levels of the constituent materials of an ITO/PEDOT/P3HT/Al hole-only device (under non-equilibrium conditions). Electrode work functions are both in the lower half of the HOMO-LUMO gap of P3HT.

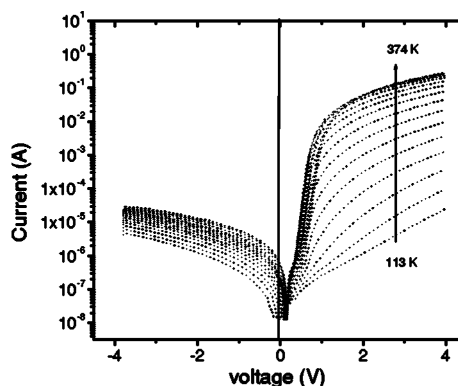

FIG. 4. Current-voltage characteristics of an 85 nm thick ITO/PEDOT/P3HT/Al device for a temperature range of 113 to 374 K at ~15 K steps, in semilogarithmic scale. A rectification factor of $\sim 5\times 10^5$ was observed at ±4 V, 304 K.

where $f(l)\rightarrow 0.5$, which corresponds to low temperature, and decreases for small l reaching its minimum when $f(l) = (8/9)$. Thus, from the $J(V)$ characteristics obeying a power law, one may estimate the characteristic energy of the exponential distribution of traps, the trap density at E_t, and at the conduction band edge, and indeed at any energy level within the band gap, the total trap density, the quasi-Fermi level, and the activation energy.

II. MATERIALS AND METHODS

The 98% regioregular P3HT, and PEDOT:PSS used in this work were purchased from Rieke Inc., and from Bayer AG, Germany, respectively. They are from the same batches used for bulk heterojunction polymer-fullerene solar cells employing P3HT as an electron donor, and a fullerene derivative, [6,6]-phenyl-C61 butyric acid methyl ester (PCBM), as an electron acceptor, showing efficiencies above 3%, at 100 mW/cm, 300 K, white light.[25]

The energy level diagram of the studied ITO/PEDOT/P3HT/Al devices (under non-equilibrium conditions) is shown in Fig. 3. The inset shows the formula of P3HT. The HOMO of P3HT has been estimated to range between −5.1 and −5.2 eV, from an SCLC analysis of hole-only thin film devices,[26] cyclic voltametry,[27] and photoelectron spectroscopy.[28]

The energy gap estimated from absorption spectroscopy is about 2.1 eV, therefore the lowest unoccupied molecular orbital (LUMO) is about −3.0 eV. However, we note that a rigorous estimate of the energy band gap should also include the exciton binding energy, which is usually a few tenths of an eV. The work functions of ITO, PEDOT, and Al are about −4.7, −5.0, and −4.3 eV, respectively. The ITO/PEDOT/P3HT/Al device is, therefore, a hole-only device since in both directions of current flow, the hole injection barrier is smaller than the electron injection barrier.

The high work function electrode was patterned by etching commercial ITO coated glass substrates in acid. The substrates were cleaned in deionized water, acetone, toluene, and isopropanol, respectively, in a hot ultrasonic bath before plasma etching in oxygen. A PEDOT:PSS water based solution was spin coated in a glove box, and the films were dried by heating the substrates on a hot plate. After cooling down the substrates, a chloroform-toluene based polymer solution (P3HT, 10 mg/ml) was then spin-coated in the nitrogen atmosphere of a glove box, O_2, 2 ppm and H_2O, 0.01 ppm. The metal top electrode (Al) was deposited by thermal evaporation in high vacuum, better than 5×10^{-7} mbar at a rate of about 0.2 nm/s.

A total of 12 devices made in different batches were studied. All devices were stored in nitrogen atmosphere prior to measurement. Dark, temperature dependent, current-voltage characteristics were then obtained by utilizing a dc current-voltage Source/Monitor Unit (Advantest TR 6143), as a voltage source and current monitor, with the device placed in a liquid-nitrogen-cooled cryostat at high vacuum of better than 10^{-5} mbar in all cases. The temperature range studied was from 113 to 374 K, and the temperature was allowed to stabilize for 3 minutes within ±0.01 K before measurement was initiated. In all cases the voltage sweep was from negative to positive voltages. No hysteresis was observed in the $J(V)$ curves at low temperatures when sweeping the voltage from negative to positive, and back to negative, but at temperatures close to and higher than room temperature, this was observed, possibly due to the irreversible thermal dedoping of impurities like remnant solvent, water and oxygen. The thicknesses of the devices were obtained by using an atomic force microscope (Burleigh Vista-100 Scanning Probe Microscope).

III. RESULTS AND DISCUSSION

Figure 4 shows typical dark current-voltage $[I(V)]$ characteristics of as-cast ITO/PEDOT/P3HT/Al hole-only devices of 85 nm thickness in the semilogarithmic scale, in the 113 to 374 K temperature range. High rectification factors of about 5×10^5 were observed in the −4 V to +4 V voltage range at 304 K.

We note that the shape of the curves remained consistent for samples prepared together, and also in separate batches, although the absolute current values varied from sample to sample, the mobilities, charge carrier density, and conduc-

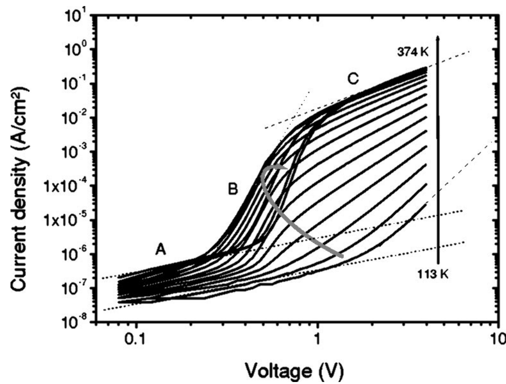

FIG. 5. Forward (+ on ITO) dark $J(V)$ characteristics of an ITO/PEDOT/P3HT/Al device (thickness $d=85$ nm) in double logarithmic scale. Region A has slope=1, corresponding to ohmic conduction, region B has slope >2, corresponding to trap filling. The log-log plot at high applied voltage (region C) has a slope=2 and is described by TFSCLC, Eq. (13). This applies only for temperatures above 287 K, otherwise slope >2, and increases with decrease in temperature.

tivities are quite comparable for all devices, for the same measurement temperatures.

The curves of Fig. 4 are replotted as current density vs voltage [$J(V)$] in a double logarithmic representation, in Fig. 5, corresponding to hole injection through the ITO/PEDOT electrode (forward bias).

At low temperatures, one identifies two different slope regions indicated in Fig. 5 by the dotted (slope=1) and dashed (slope>2) lines. As temperature increases, an intermediate region with high slope, which increases with temperature, is observed. The curves then tend to level off to some constant slope. The dashed lines are a guide for the eye, and they indicate a decrease of slope with increase in temperature. Below 286 K, the slope is greater than 2, and for temperatures above 286 K, the slope is ~2. Note that slope >2 may indicate the filling of traps distributed exponentially in energy. We may approximate that above 286 K, trap free space charge limited conduction is achieved.

Further we remark on the change of tendency to increase current as temperature is increased observed at temperatures above 321 K (see curved arrow in Fig. 5). This is explained as originating from the evaporation of remnant solvent, water, and oxygen de-doping, which tends to reduce the conductivity of the P3HT.[29] The exponential trap filling region becomes steeper, suggesting a clearer definition of trap energy levels (see Sec. I). Shallow traps which were filled by low voltages seem to have disappeared, as trap filling starts at higher voltages the higher the temperature. The discussion in this paper is valid for the temperatures below 321 K. The electrical properties of P3HT are modified permanently at higher temperatures, due to thermal annealing effects, details of which are a subject of further study.

A. Trap free space charge limited current

The topmost curve of Fig. 5 shows a plot of the forward current density voltage characteristics of an ITO/PEDOT/P3HT/Al device at 304 K in double logarithmic scale.

One can distinguish three regions, denoted A, B, and C in Fig. 5, corresponding to ohmic, trap filling and space charge limited current, respectively.

In region A ($V<0.3$ V), applied external electric field is small. The interface barrier blocks charge injection, hence the number of charge carriers participating in the current does not increase. Current depends exclusively on applied field, and on the conductivity of the material. Conduction is due to the intrinsic thermally generated charge carriers, as well as to some charges associated with the dopants, and should obey Ohm's law. For ohmic conduction the slope of log J vs log V is equal to 1. Hence in the mentioned range of voltages, Ohm's law is satisfied for these devices.

We denote region B ($0.3\ \mathrm{V}<V<0.7\ \mathrm{V}$) as the charge injection limited and trap filling region. Applied voltage has passed the threshold of blocking. The number of charges participating in the total current increases with increase in voltage. The bulk material is able to accommodate this increase in charge carriers. We understand this as the filling of hole traps within the bulk. Rapid increase in current with small increases in voltage is due to this increase in charge carrier density in the bulk. Region B is characterized by slope >2. This is usually described by the power law which assumes the filling of traps distributed exponentially within the band gap, the maximum density being at the band edge. If the trap distribution is discrete, then the curve is vertical in region B. The slope therefore can be used as a criterion for comparison of the stretching of the exponential distribution. Low slope implies gradual (extended) distribution, while higher slope indicates abrupt distribution. This region is also described by the Schockley diode equation[30] where current depends exponentially on voltage—in that case the abruptness or spread is expressed in the ideality factor.

At some voltage (near 0.7 V), all existing trapping centers are occupied by injected charge carriers, and the material starts to resist any further injection if the mobility is so low that the extra injected charges cannot be swept to the collecting electrode at the same rate at which they are being injected. Space charge then accumulates near the injecting electrode and creates a field impeding further injection. The rate of increase of current with voltage decreases, until it becomes constant again when all traps are occupied. Trap free space charge limited current should then flow.

Region C ($V>0.7$ V) of our $T=304$ K curve corresponds to trap free space charge limited current region (TFSCLC) since the obtained slope in the double log plot is equal to 2. TFSCLC can be described by Child's law,[14]

$$J = q\epsilon\epsilon_0\mu_p\frac{V^2}{d^3}. \tag{13}$$

Note that this law does not necessarily imply the absence of traps in the material, but rather that they are all filled. We fitted our experimental data corresponding to temperatures where the $J(V)$ exhibited slopes=2, i.e., between 287 and 374 K, to Eq. (13), considering $\epsilon=3$, and calculated the mobility under space charge limitation of current. Figure 6 shows the calculated mobilities.

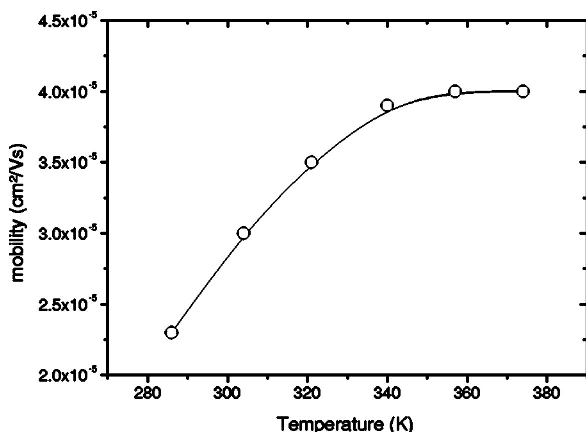

FIG. 6. Hole mobilities in an ITO/PEDOT/P3HT/Al device under forward bias, obtained from TFSCLC fits using Eq. (13) are represented as a function of temperature. Slope 2 was obtained only for temperatures between 287 and 374 K.

We note that when TFSCLC is achieved, both the contact barrier and built in fields are negligible, and the obtained mobility depends only on the properties of the bulk. We obtained a space charge limited hole mobility of 3×10^{-5} cm/V s at 304 K, which tended to a constant value of 4×10^{-5} cm^2/V s for higher temperatures. This saturation is believed to be an artefact of thermal annealing, which dedopes P3HT of oxygen and consequently reduces its conductivity.[29,31] Further we remark that it is also possible that there can still be a discrete trap level that is not filled within the experimental range of the Fermi level, and therefore that in fact the obtained mobility values can be lower than the real TFSCLC values.

B. Trap limited SCLC

The intermediate region of the $J(V)$ curves of Fig. 4(b) (region B) may be described as a trap filling regime. When the slope is greater than 2, as has been observed in this case, one may use the power law $J\sim V^m$, with $m>2$, to determine the trap energy levels, the trap densities, the total trap density, the activation energy and the quasi-Fermi energies as has been described in Sec. I B.

The slopes, m, of the double logarithmic $J(V)$ curves of Fig. 5 have been used to calculate the characteristic trap energy levels, E_t, in the band gap of P3HT. We replotted Fig. 5 and produced the straight lines to high voltages for all temperatures at which the log J-log V slope is greater than 2. It can be seen clearly in Fig. 7, that the lines meet at some common point, designated as V_c (see Sec. I). This is the critical voltage, at which current becomes independent of temperature, all traps are filled and conduction takes place in the valence band. Beyond V_c, trap free space charge limited current should flow, independent of temperature.

The inset shows the blown up crossover point(s) of plots of the straight-line-fit equations to curves of Fig. 7. We obtained that the crossover actually takes place within a narrow range of voltages between 58 and 63.2 V, and used the midpoint of $V_c=60.6$ V for the estimation of traps. The spread

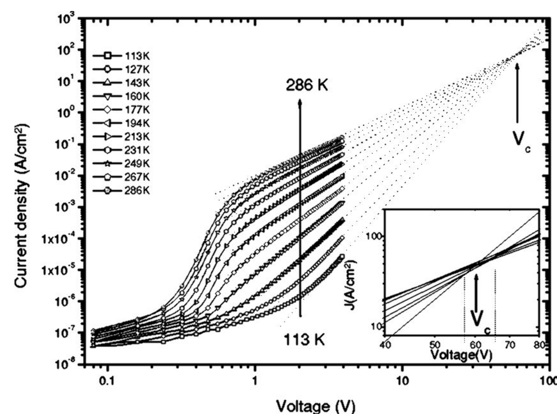

FIG. 7. The straight segments of the $J(V)$ characteristics satisfying the power law $J\sim V^m$, with $m>2$ produced all meet at a critical voltage V_c, where current is independent of temperature. The slope, m, decreases with increasing temperature. The inset shows a blown up crossover point indicating that it is actually a small range of voltages, the midpoint of which has been considered as V_c.

stems from the fact that V_c is temperature specific (see Sec. I B). Substituting it in Eq. (12), gives the total trap density to be within the range 2.81×10^{16} to 3.56×10^{16}cm^{-3}, considering the two extremes of $f(l)$. Kumar *et al.*[23] estimated the whole term with l in Eq. (12) to be about 0.5 (within 4%). Nikitenko *et al.*[32] found a fitting minimum deep trap density of 1.5×10^{16} cm^{-3} in their P3HT films when they considered a Gaussian distribution of states.

Extrapolation of the straight line fit to the calculated E_t vs T plot (not shown) yields the trap energy at absolute zero temperature. This energy corresponds to the activation energy and is equal to 0.054 eV. At $T>0$ K, E_t represents activation energy at the temperature in question.

The number of traps at the characteristic energy that marks the width of the trap distribution decreases with increase in trap depth in such a way that the product

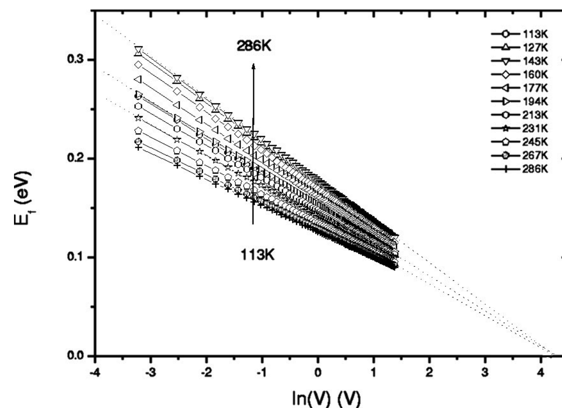

FIG. 8. At constant temperature the quasi-Fermi energy varies linearly with the natural logarithm of applied voltage. When the quasi-Fermi level coincides with the valence band edge, all the curves meet at a critical voltage V_c, at which all traps are filled, and conduction takes place through the valence band states thereafter. At V_c, current is independent of temperature.

$N(E_t)\times E_t$=constant=(N_{total}/e), from Eq. (3). The trap density at the valence band edge at any temperature differs from $N(E_t)$ by a constant multiplier, e, therefore it also decreases with increase in temperature. This can be interpreted as the filling of traps close to the valence band. Raising the temperature fills up shallow energy traps close to the valence band. Therefore, E_t is pushed further into the band gap, but there are fewer traps situated at that energy level.

By substituting the obtained total trap density in Eq. (5), we determined the position of the quasi-Fermi level as a function of temperature and of applied electric field. Figure 8 shows that the quasi-Fermi level is linearly dependent on $\ln V$, in conformity with theory [see Eq. (7)]. According to Eq. (7), the voltage at which E_F=0 eV, differs only by $f(l)$ for all temperatures. If $f(l)$ varies only slightly, then the straight lines tend to converge at V_c, as shown in Fig. 8. We note that this is the critical voltage at which the current becomes independent of temperature, the Fermi level coincides with the valence band edge, and all traps are filled. Therefore, applying V_c provides sufficient energy equal to the amount of energy that must be supplied to the material in order to fill all the traps, so that any subsequent conduction of current takes place in the valence band. Beyond that critical voltage, current conduction should be trap free, independent of temperature. We note therefore, that both voltage and heat can contribute to the filling up of traps.

IV. CONCLUSIONS

Bulk transport properties of P3HT were studied in a hole only device. The exponential trap distribution model has been briefly described, and an expression for the calculation of the total trap density was deduced, clarifying the limiting values of a prefactor that defines the validity of the model. The deduced expression yielded reasonable agreement with our experimental $J(V)$ data. The total deep hole trap density was estimated to be 5×10^{16} cm^{-3}, and the activation, energy at absolute zero temperature, was obtained to be 54 meV. A hole mobility of 3×10^{-5} cm^2/V s, at 304 K was also estimated under trap-free space charge conditions.

ACKNOWLEDGMENTS

The authors acknowledge the Geselschaft fuer Technische Zusamenarbeit (GTZ), the Deutscher Akademischer Austauschdienst (DAAD), and the German Ministry for Education and Research (BMBF) (Project Nos. 01SF0026, 01SF0119) for funding of this work.

---

*Electronic address: zivayi_chiguvare@Yahoo.com; on leave from the University of Zimbabwe, Renewable Energy Programme, P.O. Box MP 167, Mount Pleasant, Harare, Zimbabwe.

†Corresponding author. Electronic address: dyakonov@uni-oldenburg.de

[1] J. Shinar, *Organic Light Emitting Devices: A Survey* (American Institute of Physics, New York, 2002).

[2] C. J. Brabec, V. Dyakonov, J. Parisi, and N. S. Sariciftci, *Organic Photovoltaics: Concepts and Realization* (Springer-Verlag, Berlin, 2003), Vol. 60.

[3] T. Markvart and L. Castaner, *Practical Handbook of Photovoltaics, Fundamentals and Applications* (Elsevier Science, New York, 2003).

[4] C. D. Dimitrakopoulos and J. D. Mascaro, IBM J. Res. Dev. **45**, 11 (2001).

[5] S. S. Pandey, W. Takashima, S. Nagamatsu, T. Endo, M. Rikukawa, and K. Kaneto, Jpn. J. Appl. Phys. **39**, 94 (2000).

[6] Z. Bao, A. Dodabalapur, and A. J. Lovinger, Appl. Phys. Lett. **69**, 4108 (1996).

[7] H. Sirringhaus, P. J. Brown, R. H. Friend, M. M. Nielsen, K. Bechgaard, B. M. W. Langeveld-Voss, A. J. H. Spiering, R. A. J. Janssen, E. W. Meijer, P. Herwig, and D. M. de Leeuw, Nature (London) **401**, 685 (1999).

[8] A. Ullmann, J. Ficker, W. Fix, H. Rost, W. Clemens, I. McCulloch, and M. Giles, Mater. Res. Soc. Symp. Proc. **665**, 265 (2002).

[9] F. Padinger, R. S. Rittberger, and N. S. Sariciftci, Adv. Funct. Mater. **13**, 1 (2003).

[10] P. Schilinsky, C. Waldauf, and C. J. Brabec, Appl. Phys. Lett. **81**, 3885 (2002).

[11] H. Sirringhaus, N. Tessler, and R. Friend, Science **280**, 1741 (1998).

[12] T. van Woudenbergh, P. W. M. Blom, M. C. J. M. Vissenberg, and J. N. Huiberts, Appl. Phys. Lett. **79**, 1697 (2001).

[13] K. C. Kao and W. Hwang, *Electrical Transport in Solids, With Particular Reference to Organic Semiconductors*, Vol. 14 of International Series in the Science of the Solid State (Pergamon, Oxford, 1981).

[14] M. A. Lampert and P. Mark, *Current Injection in Solids* (Academic, New York, 1970).

[15] V. I. Arkhipov, P. Heremans, E. V. Emilianova, G. J. Adiaenssens, and H. Baessler, Appl. Phys. Lett. **92**, 7325 (2002).

[16] H. Baessler, Phys. Status Solidi B **175**, 15 (1993).

[17] A. J. Campbell, M. S. Weaver, D. G. Lidzey, and D. D. C. Bradley, J. Appl. Phys. **84**, 53 (1998).

[18] P. W. M. Blom and M. C. J. M. Vissenberg, Mater. Sci. Eng., B **27**, 6737 (2000).

[19] W. Bruetting, S. Berleb, and A. G. Muckl, Org. Electron. **2**, 1 (2001).

[20] S. C. Jain, W. Geens, A. Mehra, V. Kumar, T. Aernouts, J. Poortmans, R. Mertens, and W. Willander, J. Appl. Phys. **89**, 3804 (2001).

[21] V. Kumar, S. C. Jain, A. K. Kapoor, W. Geens, T. Aernauts, J. Poortmans, and R. Mertens, J. Appl. Phys. **82**, 3245 (2003).

[22] R. D. Gould and B. A. Carter, J. Phys. D **16**, L201 (1983).

[23] V. Kumar, S. C. Jain, A. K. Kapoor, J. Poortmans, and R. Mertens, J. Appl. Phys. **94**, 1283 (2003).

[24] S. J. Tans, R. G. Miedema, L. J. Geerligs, C. Dekker, J. Wu, D. Neher, and D. Wegner, Nanotechnology **14**, 1043 (2003).

[25] I. Riedel and V. Dyakonov, Phys. Status Solidi A **201**, 1332 (2004).

[26] D. Chirvase, Z. Chiguvare, M. Knipper, J. Parisi, V. Dyakonov,

and J. C. Hummelen, J. Appl. Phys. **93**, 3376 (2003).
[27] R. Valaski, L. M. Moreira, L. Micaroni, and I. A. Hummelgen, J. Appl. Phys. **92**, 2035 (2002).
[28] M. Onoda, K. Tada, A. A. Zakhidov, and K. Yoshino, Thin Solid Films **331**, 76 (1998).
[29] B. A. Mattis, P. C. Chang, and V. Subramanian, Mater. Res. Soc. Symp. Proc. **771**, L10.35.1 (2003).
[30] S. M. Sze, *Semiconductor Devices* (Wiley, New York, 1981).
[31] D. B. A. Rep, B. H. Huisman, E. J. Meijer, P. Prins, and T. M. Klapwijk, Mater. Res. Soc. Symp. Proc. **660**, JJ7.9.1 (2001).
[32] V. R. Nikitenko, H. Heil, and H. von Seggern, J. Appl. Phys. **94**, 2480 (2003).